J. Membrane Biol. 140, 1–12 (1994)

The Journal of
Membrane
Biology

Vacuolar Chloride Regulation of an Anion-selective Tonoplast Channel

P.J. Plant, A. Gelli, E. Blumwald

Department of Botany and Centre for Plant Biotechnology, University of Toronto, 25 Willcocks St., Toronto, Ontario, Canada, M5S 3B2

Received: 28 July 1993/Revised: 31 January 1994

Abstract. Fluctuations in intravacuolar chloride concentrations affected the tonoplast inward (anion flux into the vacuole) currents of sugar beets (*Beta vulgaris*). Rising vacuolar chloride concentrations induced increases in the levels of nitrate, acetate and phosphate inward currents. These currents, evoked at physiological vacuolar potentials, showed a linear relationship with the concentration of vacuolar chloride between 6 and 100 mM. Single channel currents revealed that rises in vacuolar chloride increased the frequency and probability of channel openings at a given tonoplast potential by reducing the mean closed time of the anion channel. In addition, there was an increase in the gating charge for the channel and a decrease in the free-energy favoring the transition of the channel from the closed to the open state. Vacuolar chloride had a very different effect on malate currents. Increasing chloride concentrations resulted in decreased frequency and open probability of the channel openings, a decrease in the gating charge and an increase in the mean closed time of the channel. Our results support the role for vacuolar chloride concentrations regulating the influx of anions into the vacuole, in addition to osmoregulation. The activation of channel activity by chloride will provide a pathway for the storage of nutrients, such as nitrate and phosphate into the vacuole, while the reduction of the malate currents will allow the use of malate for mitochondrial oxidation and cytoplasmic pH control.

Key words: Anion channels — Patch clamp — Beet vacuoles — Chloride regulation — Inward currents — Tonoplast

Correspondence to: E. Blumwald

Introduction

Ion transport plays a critical role in a number of biological processes. In animal cells, ion channels are involved in the mediation of cell excitability, inter/intracellular communication, neural transmission and the regulation of cell volume, in addition to other metabolic processes (Franciolini & Petris, 1990; Neher, 1992; Sakmann, 1992). Similarly, ion transport in higher plants plays a key role in many processes including cell volume regulation, inter/intracellular communication and detoxification of the cytoplasm (Pantoja et al., 1992; Wink, 1993). Vacuolar membrane (tonoplast) transport specifically plays a key role in the control of cytoplasmic homeostasis and cell osmoregulation (Boller & Wiemken, 1986).

Tonoplast channels for passive ion movement of varying degrees of specificity are ubiquitous in plant cells (Hedrich, Schroeder & Fernandez, 1987; Tyerman, 1992). These channels are essential for the control of the vacuolar membrane potential. The movement of ions down their electrochemical potential not only serves as a pathway for the storage and retrieval of nutrients, but also as a means for polarizing/depolarizing the tonoplast potentiation, which in turn would serve as a regulatory mechanism for the activity of the tonoplast H^+ pumps (Blumwald, 1987).

Ion channel transport across the tonoplast has been previously characterized (Coyaud, Kurdjian & Hedrich, 1987; Hedrich & Neher, 1987; Hedrich & Kurkdjian, 1988; Pantoja et al., 1992), and several distinct types of channels involved in anion transport were identified. At low cytoplasmic Ca^{2+} concentrations ($<10^{-6}$ M), ion conductance occurs predominantly through instantaneously activated fast-vacuolar type (FV-type) channels. These channels display a low conductance and low selectivity for anions (Hedrich & Neher, 1987). In contrast, slow-vacuolar type (SV-type) channels account-

ed for all ion conductances at high cytoplasmic Ca^{2+} concentration ($>10^{-6}$ M). These channels were strongly voltage dependent and had similar selectivities for cations and anions (Hedrich & Neher, 1987). In addition, an anion channel was characterized in vacuoles from *Beta.* Currents evoked at low cytoplasmic Ca^{2+} were time dependent, had a high selectivity for anions and were proposed to play a role in vacuolar malate transport (Pantoja et al., 1992).

In a moderate halophyte such as sugar beet (*B. vulgaris*) the tonoplast plays a crucial role in regulating anion fluxes into the vacuole where high concentrations of NaCl are accumulated. Inorganic ions such as Cl^- are compartmentalized in the vacuole in concentrations up to 300 mM (Matile, 1978) and play a significant role in osmoregulation. Inorganic anions such as nitrate, phosphate, acetate, malate and chloride are essential for plant growth, yet little is known of the physiological mechanisms which can regulate the transport and compartmentalization of these ions. To date, few mechanisms of control have been found for tonoplast channels aside from the regulation by cytoplasmic Ca^{2+} (Hedrich & Neher, 1987) and by cytoplasmic Cl^- (Pantoja et al., 1992). Fluctuations in cytoplasmic Ca^{2+} concentrations were shown to play a role in the activation and deactivation of the SV- and FV-type channels (Hedrich & Neher, 1987). Cytoplasmic chloride concentrations were also shown to affect the operation of the SV-type vacuolar channel. High chloride concentrations activated ion currents that mediated the transport of cations into the vacuole (Pantoja et al., 1992). Here, we provide evidence that vacuolar chloride may provide a regulatory mechanism for the transport of anions into the vacuole through a channel selective for anions, suggesting a multifunctional role for this halide as it is stored in the vacuole.

Materials and Methods

Plant Material

Cell cultures of sugar beet (*B. vulgaris*) were grown as previously described (Blumwald & Poole, 1987). Cells were grown in media containing 25 mM NaCl. Vacuoles of 25–30 μm in diameter were isolated by osmotic shock as formerly described (Pantoja, Dainty & Blumwald, 1989).

Experimental Solutions

In all experiments, the composition of the bathing solution (cytoplasmic side) was: 2 mM $MgCl_2$, 1 mM $CaCl_2$, 1.1 mM BAPTA to give a final concentration of 1 μM free Ca^{2+}, 5 mM Tris/Mes, pH 7.5 and 50 mM of either $(NMDG)_2$malate, (NMDG)-NO_3, (NMDG)-Acetate or $(NMDG)_2HPO_4$. The vacuolar interior was simulated with pipette-filling solutions containing: 2 mM $MgCl_2$, 1 mM $CaCl_2$, 5 mM Tris/Mes, pH 6.0 and either 50 mM or 100 mM (NMDG)-Cl with 5 mM of either $(NMDG)_2$malate, (NMDG)-NO_3, (NMDG)-Acetate or $(NMDG)_2HPO_4$. The osmolarity of both the pipette and bathing solutions was adjusted to 450 mOsmol with D-sorbitol. NMDG (*N*-methyl-D-glucamine) was used as a counterion to assure that there would be no contribution to the overall vacuolar current by this ion, as NMDG is not transported across the tonoplast. The bi-ionized forms of malate and phosphate were only considered in the pH range used, since the activity of the mono-ionized form was less than 10% (malate) and 5% (phosphate) of the activity of the bi-ionized form.

Electrophysiology

Conventional patch clamp techniques were used to measure ionic currents across the vacuolar membrane (tonoplast) in whole-vacuole and isolated inside-out patch configurations (Hamill et al., 1981). Recording pipettes were prepared from borosilicate glass capillaries (Drummond Scientific, Broomall, PA), pulled in two stages with a vertical pipette puller (Narishige, Tokyo, Japan), heat-polished for 3–4 min and coated with a layer of silicone (Sigmacote, Sigma). Electrode resistances ranged from 3 to 8 mΩ, depending on the pipette geometry and the type of solutions used. Gigaohm seals (varying from 3–15 MΩ) between the electrode and the tonoplast were obtained by application of gentle suction to the patch pipette. Applying a voltage pulse of 1 volt for 30 msec broke the tip-spanning portion of the membrane resulting in the whole-vacuole configuration. To minimize liquid junction potentials while recording, the reference electrode contained an identical solution to that used in the bathing solution. Liquid junction potentials were calculated as described previously (Barry & Lynch, 1991) and clamp voltages were adjusted accordingly. The whole vacuole steady-state currents that were obtained by 5 sec voltage pulses were used in establishing vacuolar current-voltage (*I-V*) relationships. The tonoplast potential was held at 0 mV and pulses of ±20 mV were alternately incremented every 10 sec up to ±100 mV. Outside-out patches were obtained from the whole-vacuole configuration by pulling the recording pipette away from the vacuole (Hamill et al., 1981). Vacuolar currents were obtained with the pCLAMP program (version 5.0, Axon Instruments, Foster City, CA), and data were stored in a PCII-386 computer operating on-line.

Both whole-vacuole and single channel currents were recorded with a 3,900 integrated patch clamp system (Dagan, Minneapolis, MN) and were filtered at 500 Hz (whole vacuole) and 200 Hz (single channel) with an internal four-pole Bessel filter at 22 ± 2°C. Capacity and series resistance compensation (whole-vacuole configuration) was done with the system circuitry. Pulses from single channel traces were digitized at 44 Hz by a pulse code modulator and stored on videotape (DAS 900, Dagan, Minneapolis, MN). All single channel data were digitized, processed and analyzed with the pCLAMP program.

Single Channel Kinetics

The estimates of mean open and closed times of single channel records with the presence of more than one channel were made by following the methods of Labarca, Coronado & Miller (1980). This approach assumes the membrane patch contains channels that are identical and independent, with each channel having one open and one closed state. We assumed that the channels followed the simple kinetic scheme:

$$open \underset{k_-}{\overset{k_+}{\leftrightarrows}} closed$$

where k_- is the rate constant of closing for the open channel and k_+ the opening rate constant of the channel in the closed state.

Each rate constant k_+ and k_- can be obtained by fitting exponentials to the histograms of time intervals (dwell histograms) in which precisely n channels are open or N-n channels are closed with N being the total number of channels in the patch. These constants are assumed to be the reciprocals of the mean open and mean closed times of an individual channel.

The mean closed time of the channel assembly (the mean time spent in the state in which all the channels are closed) is $1/k_o$, where $k_o = Nk_-$. Similarly, the mean time being spent with n channels in the open state and $N - n$ channels closed is $1/k_n$ where $k_n = (N - n)k_- + nk_+$. In practice, the number of channels (N) is estimated from the observed number of current levels in the single channel record and the probability of a channel being open is estimated from:

$$P_{\text{open}} = \sum_{n=1}^{N} \frac{nP_n}{N}$$

where P_n is the probability that n channels are open. This parameter is calculated directly from the mean open time ($1/k_n$) of the channels in the single channel record. More simply, values of P_{open} were calculated from the mean open and mean closed times:

$$\frac{\overline{t_{\text{open}}}}{(\overline{t_{\text{open}}} + \overline{t_{\text{closed}}})}$$

This method takes into consideration the *average* number of channels open in the patch and, as a consequence, values of N estimated from the single channel record do not affect the values of P_{open} obtained in this manner. This is relevant especially for channels with low probabilities of opening where it is difficult to obtain the correct N and the observed value is usually an underestimate.

Amplitude distribution histograms were obtained for single channel recordings at +80 mV and were also used to calculate the mean single channel open probabilities as:

$$P_o = \frac{\sum_{n=1}^{N} nt_n}{N\sum_{n}^{N} t_n}$$

where P_o is the probability that any one channel is open, t_n is the area under the histogram peaks with n open channels (Labarca et al., 1980). The estimation of P_o was subject to the assumed value of N which was estimated by the number of channels present in the single channel records. Values for P_o obtained in this manner were compared to values of P_o obtained using the mean open and closed times for the channel. Values obtained by both methods were in agreement to within 23% (t-value = 1.6, significant at the 10% level) which was satisfactory for either method to be used to approximate values of k_+ and/or k_-. All values of P_o reported in this paper are calculated using the method incorporating mean open and closed times.

The validity of this method is dependent on the assumptions that (i) there is an exponential distribution of the dwell times in each state, (ii) the reciprocal time constants of these exponentials varies linearly with the number of states (the mean time spent in the state with n channels open and N-n channels closed is $1/k_n$); (iii) n, the number of channels open can be determined from the single channel record; (iv) the channels have identical kinetics, (v) the channels are independent of each other and (vi) each channel has only one open and one closed state.

While the majority of the single channel data was fit by two exponentials in the closed state (suggesting more than one class of the closed state), the closed states of short lifetime and low probability of occurrence (closed states within bursts of channel openings) were omitted from the data (Sakmann & Trube, 1984). The dominant part of the data was explicable by the fluctuations of the channel between a single open state and a single closed state. Channel bursts were very infrequent and the total closed times within the bursts were insignificant compared to closed times between bursts.

Voltage Dependence of Steady-State Anion Currents

The two state model of channel gating predicts a whole-cell conductance-voltage relation such that the conductance of the ensemble of channels is voltage dependent (Labarca et al., 1980). This model makes the assumption that the steady-state conductance measures the average number of channels in the open state, since it expresses the thermodynamic equilibrium between the open and closed states. The total free energy of the transition from the closed to the open state is defined by two variables: the internal free energy of opening (ΔG_i) and the change in energy of the dipole moments (z) associated with the two conformational states of the protein in the electric field, according to the following relationship:

$$\ln\frac{1-\theta(V)}{\theta(V)} = \frac{\Delta G_i}{RT} + \frac{zFV}{RT}$$

where the relative conductance (θ) is defined as the ratio G/G_{max}.

Calculation of Permeability Ratios

The Goldman-Hodgkin-Katz permeability ratio was modified as by Lewis (1979) to calculate the permeability ratios of malate and phosphate relative to chloride as:

$$V = \frac{RT}{F}\ln\frac{[\text{Cl}]_i + 4\frac{P'_{\text{anion}}}{P_{\text{Cl}}}[\text{anion}]_i}{[\text{Cl}]_o + 4\frac{P_{\text{anion}}}{P_{\text{Cl}}}[\text{anion}]_o e^{\frac{EV}{RT}}}$$

where P' is defined as:

$$P'_{\text{anion}} = \frac{P_{\text{anion}}}{1 + e^{\frac{FV}{RT}}}$$

Conventions and Terminology

A recently proposed convention for electrophysiological measurements in endomembranes was used, where the vacuolar lumen is considered electrically equivalent to the extracellular space (Bertl et al., 1992). We let the potential difference or voltage across the vacuolar membrane V_m be calculated as the electric potential of the cytoplasm minus that of the vacuole. Negative or inward currents across the tonoplast represent cation flow into the cytoplasm from the vacuole or anion flow into the vacuole from the cytoplasm and are plotted downward. Conversely, positive charges leaving the cytoplasm or negative charges entering the cytoplasm are designated as positive or outward currents and are plotted upwards in all graphs.

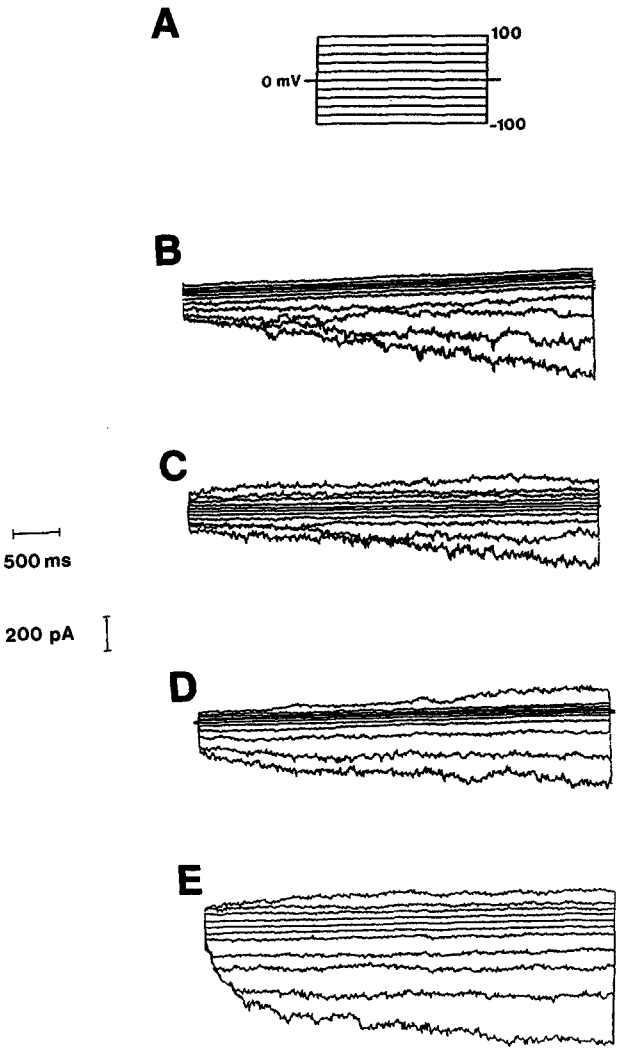

Fig. 1. Voltage clamp records from whole vacuoles of sugar beet vacuoles. The tonoplast potential was held at 0 mV and pulses of ±20 mV were alternately incremented every 10 sec up to ±100 mV (*A*). (*B*) Time-dependent inward currents (downward deflections) were evoked by negative voltage pulses with the vacuole exposed to 50 mM $(NMDG)_2$malate and 6 mM Cl^- in the cytoplasm and 5 mM $(NMDG)_2$malate and 6 mM Cl^- in the vacuole. Positive voltage pulses elicited small instantaneous outward currents (upward deflections). (*C*) When the vacuolar chloride concentration was increased to 100 mM, the magnitude of the inward currents was significantly reduced. The outward currents decreased in magnitude. (*D*) When malate was replaced with nitrate under the same conditions as *B*, negative voltage pulses evoked small time-dependent inward and instantaneous outward currents. (*E*) With an increase in vacuolar chloride to 100 mM, the inward currents markedly increased in magnitude while the outward increased.

Results

Chloride Effects on Whole-Vacuole Currents

When voltage-clamp experiments were performed under physiological conditions (cytoplasmic Ca^{2+} concentrations (10^{-6} M) and cytoplasmic and vacuolar pH, 7.5 and 6.0, respectively) application of voltage pulses ranging from a holding potential (V_h) of 0 to ±100 mV in steps of 20 mV (Fig. 1*A*), activated currents across the tonoplast (Fig. 1*B, C*). With 50 mM $(NMDG)_2$malate in the cytoplasm and 5 mM $(NMDG)_2$malate in the vacuole, negative and positive voltages stimulated instantaneous outward and time-dependent inward currents, respectively (Fig. 1*B*). When chloride (100 mM) was introduced to the vacuolar solution, the time-dependent inward currents decreased while the instantaneous currents remained largely unaffected (Fig. 1*C*). Current levels measured 4.8 sec after the onset of stimulating voltage pulses (steady-state currents) were plotted against the applied voltage (Fig. 2*A*). The magnitude of the inward currents varied with the concentration of vacuolar chloride used. Inward malate currents were markedly reduced in the presence of increasing vacuolar chloride concentrations as compared with control current levels ($[Cl^-_{vac}]$ = 6 mM). The decrease in the amplitude of the inward currents was most evident at potentials more negative than −50 mV.

When malate was substituted with nitrate, the effect of chloride was stimulatory rather than inhibitory. In the presence of 50 mM (NMDG)-NO_3 in the cytoplasm and 5 mM (NMDG)-NO_3 in the vacuolar solution, positive and negative voltages stimulated both instantaneous outward and time-dependent inward currents, respectively (Fig. 1*D*). However, when chloride was added to the vacuolar solution, the time-dependent inward currents increased in magnitude (Fig. 1*E*). Figure 2*B* shows the current-voltage (*I-V*) relationship of nitrate for the different vacuolar concentrations of chloride. In contrast to the observed decrease of the malate inward currents, rising vacuolar chloride concentrations increased the vacuolar inward currents when nitrate was present. Similar stimulatory effects of increasing vacuolar chloride concentrations on vacuolar inward current were seen using phosphate and acetate as the major anion (*data not shown*). As before, the effects of chloride were most distinctive at potentials beyond the reversal potential (E_{rev} or zero-current potential) of chloride (−50 mV).

The selectivity of the putative anion channel mediating the inward currents was determined in the presence of both high and low intravacuolar chloride. With 6 mM chloride in the cytoplasm and vacuole and a 10:1 gradient of either nitrate, acetate or phosphate (50 mM cytoplasm, 5 mM vacuole), the reversal potentials of the time-dependent inward currents ranged from −20 to −40 mV (*data not shown*). Using these values of E_{rev}, permeability ratios for P_{anion}/P_{Cl^-} were calculated using the Goldman-Hodgkin-Katz equation. Values of P_{Cl^-}/P_{Ac^-} and $P_{Cl^-}/P_{NO_3^-}$ = 10 and $P_{Cl^-}/P_{HPO_4^{2-}}$ = 20 were obtained. Under similar conditions with malate present in solution, reversal potential values between

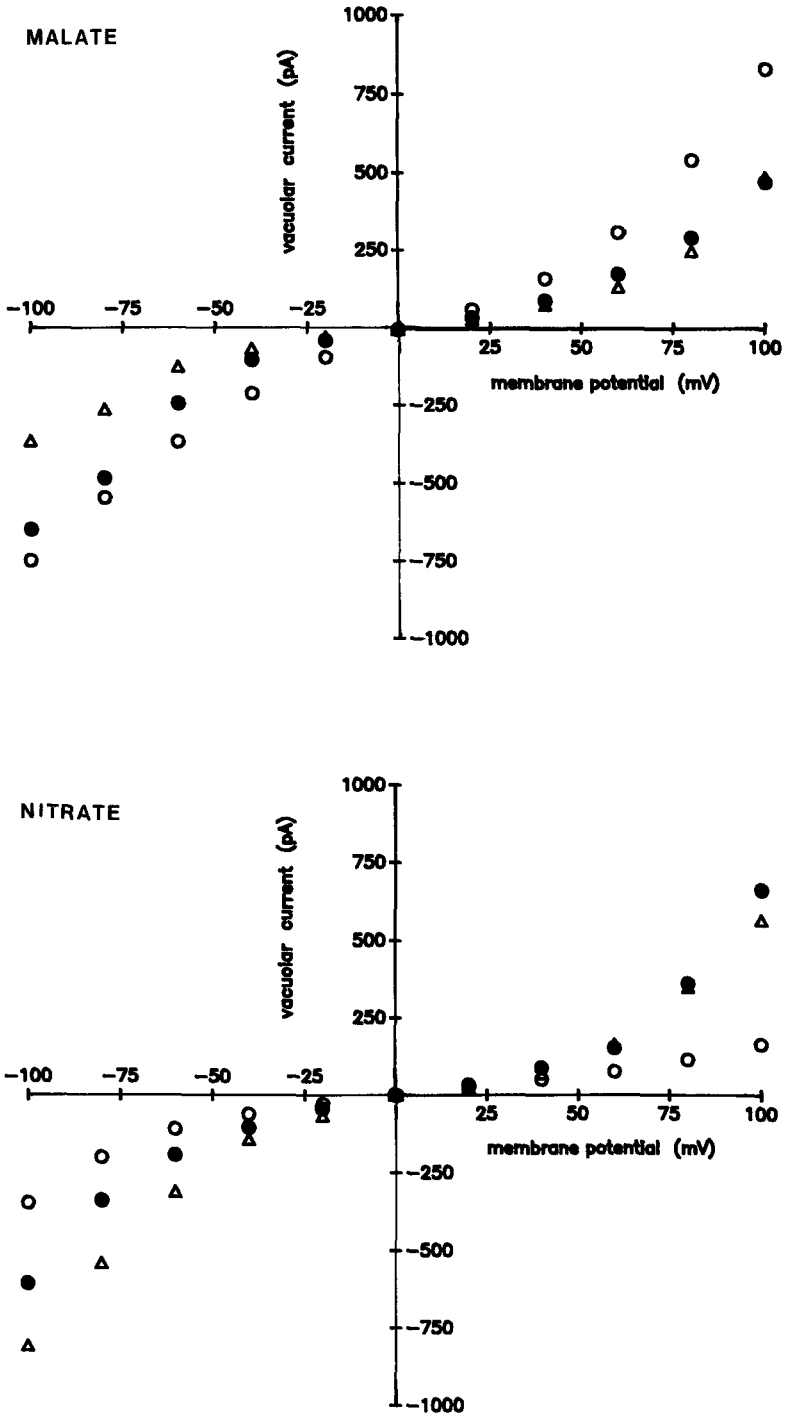

Fig. 2. The magnitude of the whole-vacuole inward currents is dependent on $[Cl^-_{vac}]$. (*Upper panel*) With malate present in solution, the large time-dependent inward currents present at low (6 mM) vacuolar chloride concentrations (○) were significantly reduced in the presence of 50 mM (●) and 100 mmM (△) vacuolar chloride at negative vacuolar potentials. (*Lower panel*) In the presence of nitrate, increasing the vacuolar chloride concentrations to 50 mM (●) and 100 mM (△) increased the magnitude of the time-dependent inward currents over those evoked at low (6 mM) $[Cl^-_{vac}]$ (○). Data points are the mean ± SE (n = 6). SE bars were equal to or smaller than the symbols used in the graph.

0 and +20 mV were obtained to give values of $P_{Cl^-}/P_{mal^{2-}} = 5$. A decreasing tonoplast permeability sequence from chloride to phosphate in the presence of low vacuolar chloride was established:

$$P_{chloride} > P_{malate} > P_{acetate} > P_{nitrate} > P_{phosphate}$$

When vacuoles were exposed to a gradient of chloride (100 mM in the vacuole, 6 mM in the cytoplasm) with 50 mM either nitrate, phosphate or acetate in the cytoplasm and 5 mM in the vacuole, time-dependent inward currents reversed at potentials between 0 and +30 mV (*data not shown*) with NO_3^-, Ac^- and HPO_4^{2-}. Values of $P_{Ac^-}/P_{Cl^-} = 7$, $P_{NO_3^-}/P_{Cl^-} = 4$ and $P_{HPO_4^{2-}}/P_{Cl^-} = 1$ were obtained. Slightly more negative reversal potentials ($E_{rev} = -20$ to -30 mV) were obtained with malate in solution and a value of $P_{Cl^-}/P_{mal^{2-}} = 5$ was calculated. A decreasing tonoplast perme-

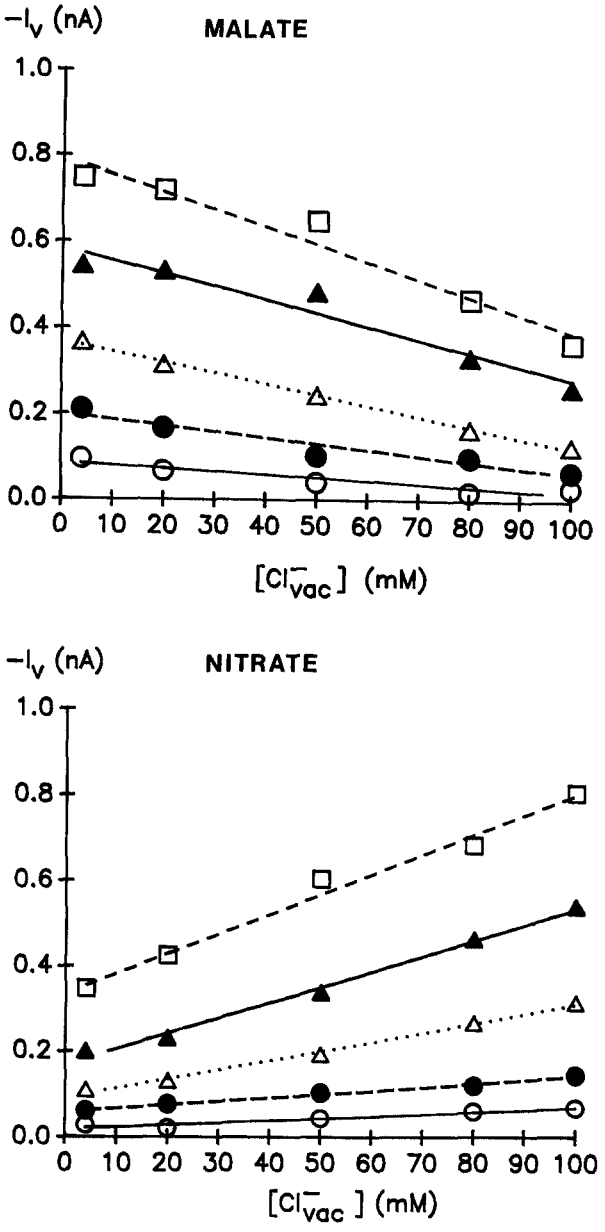

Fig. 3. *(Upper panel)* With malate present in solution, the magnitude of the time-dependent inward currents at −20 mV (○), −40 mV (●), −60 mV (△), −80 mV (▲) and −100 mV (□) decreased linearly with increasing $[Cl^-_{vac}]$ between 6 and 100 mM. *(Lower panel)* When nitrate was used in solution, the magnitude of the time-dependent inward currents at the aforementioned potentials increased linearly with rising concentrations of vacuolar chloride. Data points are the mean ± SE (n = 6). SE bars were equal to or smaller than the symbols used in the graph.

Table 1. Free energy (ΔG_i) and gating charges (z) for anion transport

Experimental solutions (mM)	ΔG_i (K_{cal}/mol)	z
50 $malate_{cyt}$/6 Cl^-_{vac}	0.90	−1.05
50 $malate_{cyt}$/100 Cl^-_{vac}	1.56	−0.69
50 $nitrate_{cyt}$/6 Cl^-_{vac}	1.82	−0.70
50 $nitrate_{cyt}$/100 Cl^-_{vac}	1.53	−1.17
50 $acetate_{cyt}$/6 Cl^-_{vac}	2.31	−0.76
50 $acetate_{cyt}$/100 Cl^-_{vac}	1.63	−1.06
50 $phosphate_{cyt}$/6 Cl^-_{vac}	1.87	−0.35
50 $phosphate_{cyt}$/100 Cl^-_{vac}	1.10	−1.19

Values were calculated from Boltzmann plots of whole-vacuole currents as described in Fig. 4.

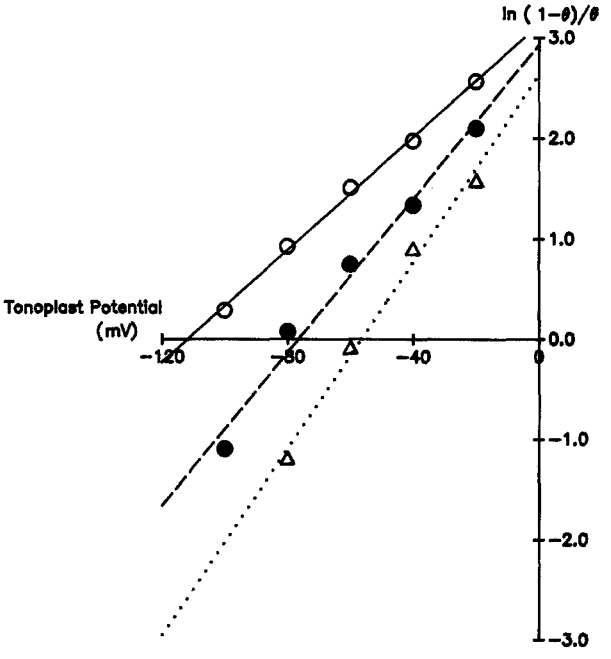

Fig. 4. Boltzmann plot of the whole-vacuole currents recorded with 50 mM NMDG-NO_3^- and 6 mM Cl^- in the bathing solution (cytoplasm) and 5 mM NMDG-NO_3^- with either 6 mM (○), 50 mM (●), or 100 mM (△) Cl^- in the pipette (vacuolar) solution. The relative conductance (θ) is defined as the ratio G/G_{max}. The slope of the least-squares fit line (z) represents the gating charge for the channel and the Y-intercept (ΔG_i) was used to calculate the free-energy (kCal/mol) of the transition from the closed to the open state.

ability sequence from acetate to malate in the presence of high vacuolar chloride was elucidated:

$$P_{acetate} > P_{nitrate} > P_{phosphate} > P_{chloride} > P_{malate}$$

The magnitude of the time-dependent inward current in the presence of malate and nitrate showed linear relationships with the vacuolar chloride concentration at all levels of tonoplast potentials tested (Fig. 3*A* and *B*). In the presence of malate the slopes of these relationships decreased as the vacuolar potential was more negative (Fig. 3*A*). With nitrate in solution the slopes in-

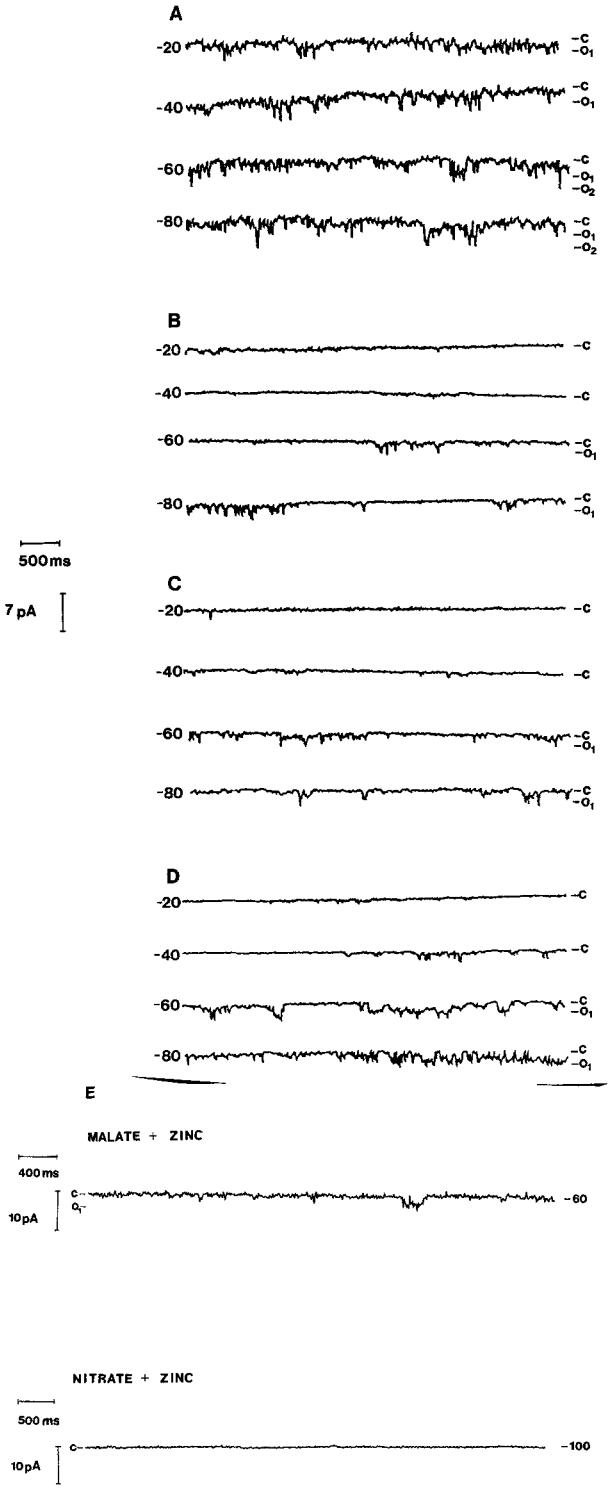

Fig. 5. Single channel currents from isolated outside-out tonoplast patches stimulated at −80 mV. With malate in solution, single channel activity was reduced with increasing concentrations of vacuolar chloride. Currents recorded with malate in solution in addition to 6 mM (*A*) and 50 mM (*B*) vacuolar chloride. Increases in vacuolar chloride concentrations stimulated channel activity. An increase in the number of single channel openings with nitrate and 6 mM vacuolar chloride (*C*) was observed when chloride concentrations were raised to 50 mM (*D*). (*E*) With the addition of 1 mM $ZnCl_2$ to the bathing solution, single channel currents evoked at low (6 mM) vacuolar chloride concentrations were reduced in the presence of malate (*Upper panel*) and were fully inhibited in the presence of nitrate (*Lower panel*).

creased with negative vacuolar potentials (Fig. 3*B*). To calculate the apparent number of chloride ions needed for the activation of the inward currents, a Hill plot was constructed using the current evoked at −100 mV as I_{max}, the maximum current value (*not shown*). The plot revealed a minimum requirement of one chloride anion for activation of the inward current (Hill coefficient = 0.8). Similar values were also obtained with Ac^- and PO_4^{2-} (*not shown*). The deactivation of malate inward currents also required a minimum of one chloride anion (Hill coefficient = 0.8) (*not shown*).

Calculations from Boltzmann plots (Table 1, Fig. 4) revealed that increasing the vacuolar chloride concentrations decreased the free energy (Gibbs free energy, ΔG_i) needed to change the channel from the closed to the open state for NO_3^-, Ac^- and HPO_4^{2-}. In addition, an increase in the vacuolar chloride concentration increased the channel gating charge (the sensitivity of the currents to the electrical field across the tonoplast, z); hence, the net negative charge moving towards the *cis* (vacuolar) side of the tonoplast when the channel opens (Labarca et al., 1980). With malate present in solution, an increase in vacuolar chloride produced an increase in the free energy coefficient and a decrease in the channel gating charge.

Steady-State Kinetics of Single Channel Currents

A detailed analysis of channel gating kinetics was obtained by statistical analysis of the current fluctuations in membrane patches where one or more channels were active. Single channel activity was studied in isolated inside-out patches from the tonoplast under the same conditions as the whole-vacuole experiments. Figure 5*A* shows part of the current records from an inside-out patch obtained at voltages from −20 to −80 mV with 50 mM $(NMDG)_2$malate with 6 mM Cl^- in the bathing solution and 5 mM $(NMDG)_2$malate with 6 mM Cl^- in the pipette solution. The voltage-dependent channel openings appeared to be grouped into complex bursts. Such an observation would indicate that the channel had more than one class of closed states (Hille, 1984). Similar results were seen when using (NMDG)-NO_3 (Fig. 5*C*), (NMDG)-Acetate and $(NMDG)_2HPO_4$ (*data not shown*).

This suggestion of multiple closed states was confirmed by the dwell histograms of the channel-closed stages (Fig. 6*B, D, F, H*). Within the range of the dwell histogram (0 − 500 msec), the distribution of the closed state duration could be fitted by a sum of two exponentials. The distribution of the channel open times is depicted by the histograms *A, C, E* and *G* in Fig. 6. All dwell histograms could be fitted by a single exponential which suggested the existence of one open state. Occasionally, obvious substates (above one-quarter open-state amplitude) were regarded as open states and were compiled with the data for the open-time dwell histograms. These substates were not frequent enough to

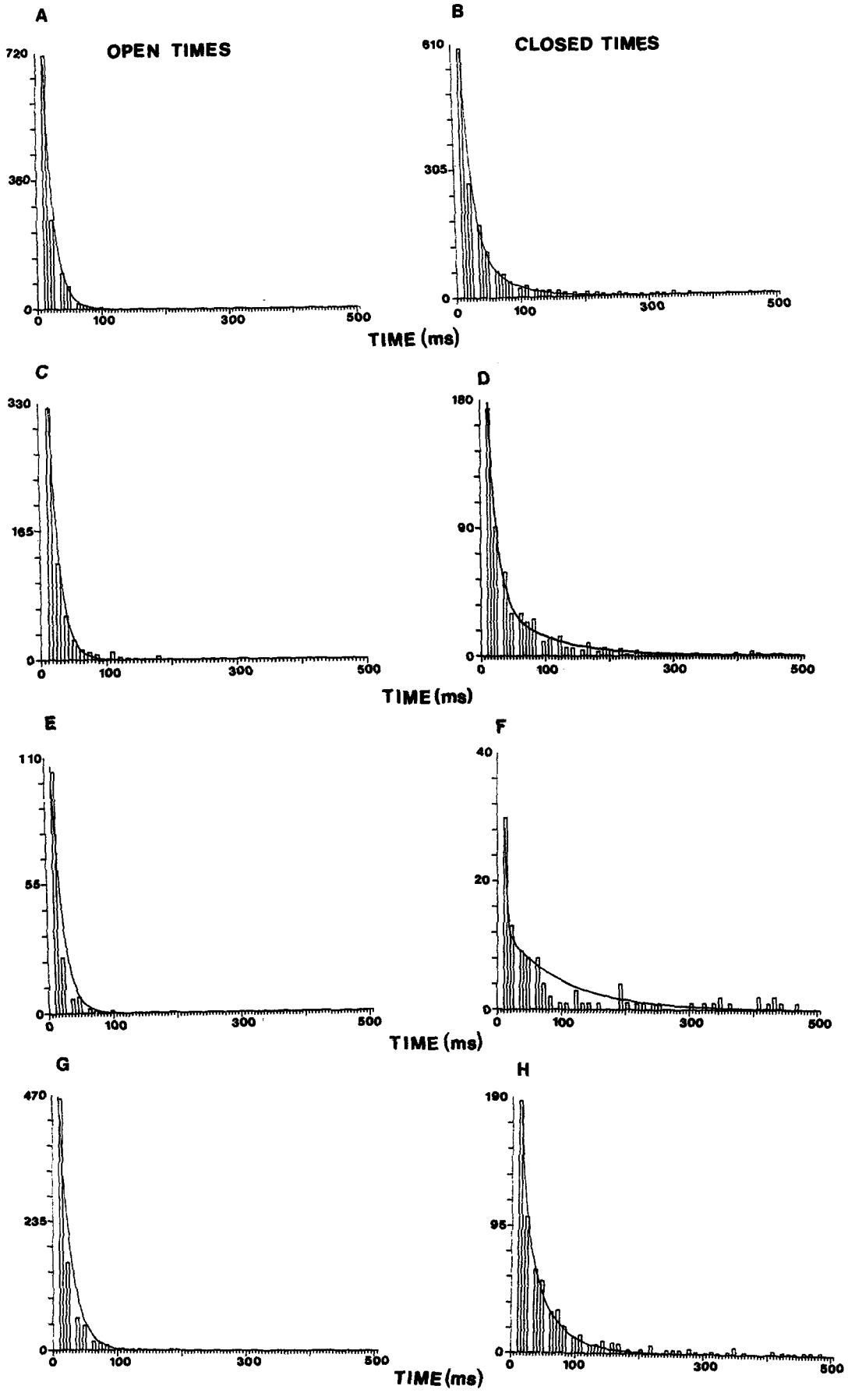
A
OPEN TIMES
720
360
0
0
100
300
500
B
CLOSED TIMES
610
305
0
0
100
300
500
TIME (ms)
C
330
165
0
0
100
300
500
D
180
90
0
0
100
300
500
TIME (ms)
E
110
55
0
0
100
300
500
F
40
20
0
0
100
300
500
TIME (ms)
G
470
235
0
0
100
300
500
H
190
95
0
0
100
300
500
TIME (ms)

Table 2. Mean single channel properties

Experimental solutions (mM)	n	g (pS)	P_{open}	Δt_{open} (msec)	Δt_{closed} (msec)
50 $malate_{cyt}$/6 Cl^-_{vac}	5	8.55	0.14	5.34	32.73
50 $malate_{cyt}$/100 Cl^-_{vac}	1	9.27	0.02	1.069	58.69
50 $nitrate_{cyt}$/6 Cl^-_{vac}	1–2	14.65	0.06	1.44	21.59
50 $nitrate_{cyt}$/100 Cl^-_{vac}	3	15.49	0.37	1.01	1.74
50 $acetate_{cyt}$/6 Cl^-_{vac}	1–2	16.61	0.084	3.08	33.55
50 $acetate_{cyt}$/100 Cl^-_{vac}	3	20.01	0.209	2.50	9.75
50 $phosphate_{cyt}$/6 Cl^-_{vac}	2	6.73	0.051	1.135	21.19
50 $phosphate_{cyt}$/100 Cl^-_{vac}	2–3	9.29	0.111	1.259	10.01

Values were calculated from single channel recordings. n = number of channels in the patch; g = conductance; P_{open} = channel open probability; Δt_{open} and Δt_{closed} = mean open and closed times, respectively.

cause a significant deviation from the single-exponential distribution that was characteristic of the open state.

The single channel openings were diminished as the vacuolar chloride concentration was increased and the vacuoles were exposed to conditions (bathing and pipette) containing malate (Fig. 5*B*). Contrary to what was observed with malate, when NO_3^- (Fig. 5*D*), Ac^- or HPO_4^{2-} (*data not shown*) were present in the experimental solutions, an increase in vacuolar chloride stimulated channel openings. Low concentrations of $ZnCl_2$ (1 mM) reduced single channel malate currents evoked in the presence of low vacuolar chloride (Fig. 5*E, Upper panel*) from the cytoplasmic side of the tonoplast and fully inhibited nitrate currents (*Lower panel*) under the same conditions.

Estimates for the mean open and mean closed times for the different anions under the varying chloride concentrations were calculated from the dwell histograms of the open and closed states. It should be noted that, for analysis, the brief gaps represented by exponentials of less than 1 msec time constants (closed times within bursts) were neglected from the data. The analysis was confined to bursts of openings and the gaps between bursts. For comparison, dwell histograms of open and closed states for both malate and nitrate with low (6 mM) vacuolar chloride (Fig. 6*A, B:* malate, Fig. 6*C, D:* nitrate) and with high (100 mM) vacuolar chloride (Fig. 6*E, F:* malate, Fig. 6*G, H:* nitrate) are shown. Rate constants are given in the figure legend. Table 2 shows that in the presence of malate, the mean closed times increased with rising concentrations of vacuolar chloride. The open time of malate channel activity with 6 mM Cl^-_{vac} (5.34 msec) was reduced with higher concentrations of vacuolar chloride (Table 2). For NO_3^-, Ac^- and HPO_4^{2-} mean closed times with 6 mM Cl^-_{vac} (1.44, 3.08 and 1.13 msec, respectively) decreased with higher concentrations of Cl^-_{vac} while the mean open times remained unchanged (Table 2).

Mean open probabilities (P_{open}) (Table 2) were calculated using the method of Labarca et al. (1980). For patches exposed to 50 mM nitrate and 6 mM chloride on the cytoplasmic side and 5 mM nitrate and 6 mM chloride on the vacuolar side, the open probability of the channel was 0.063. When vacuolar chloride was increased to 50 mM (*data not shown*) and 100 mM (Table 2), the probability increased to 0.145 and 0.367 respectively. This pattern was true of the open probabilities of Ac^- and HPO_4^{2-} as well (Table 2). The open probability of malate in solution with low (6 mM) vacuolar chloride, P_{open} (0.140), was reduced at higher concentrations of Cl^-_{vac} (0.02 for 100 mM Cl^-_{vac}).

The current-voltage relation shown in Fig. 7*A* revealed the inward single channel currents of malate at varying concentrations of Cl^-_{vac}. The plot shows that neither the magnitude of the single channel currents nor the single channel conductance (8.55 pS) was significantly changed by increasing the concentration of Cl^-_{vac}. The reversal potential (x-intercept) remained unaltered by the increase in vacuolar chloride. When malate was substituted with NO_3^- (Fig. 7*B*), Ac^- or

Fig. 6. Histograms of open and closed dwell states of the tonoplast anion channels. Histograms represent data collected from outside-out patches with malate (*A* and *B*), nitrate (*E* and *F*), and 6 mM vacuolar chloride. The vacuolar chloride concentration was then increased to 50 mM with malate (*C* and *D*) and nitrate (*G* and *H*) in solution. The open-time histograms (*A, C, E* and *G*) represent the lifetimes of the channels in a state with at least one channel open. The histograms of the closed times represent the lifetimes of all the channels in the closed state. The histograms are fit with lines of single exponentials for all the open states. Although the closed-time histograms are best fit with two exponentials, the closed state with a short lifetime and low probability of occurrence was omitted from the data. The dominant part of the data was represented by one closed state. Rate constants for the patches were 14.29 $msec^{-1}$ (open times, *A*), 50 $msec^{-1}$ (closed times, *B*), 14.29 $msec^{-1}$ (open times, *C*), 153.85 $msec^{-1}$ (closed times, *D*), 14.29 $msec^{-1}$ (open times, *E*), 90.91 $msec^{-1}$ (closed times, *F*), 18.18 $msec^{-1}$ (open times, *G*), and 40 $msec^{-1}$ (closed times, *H*).

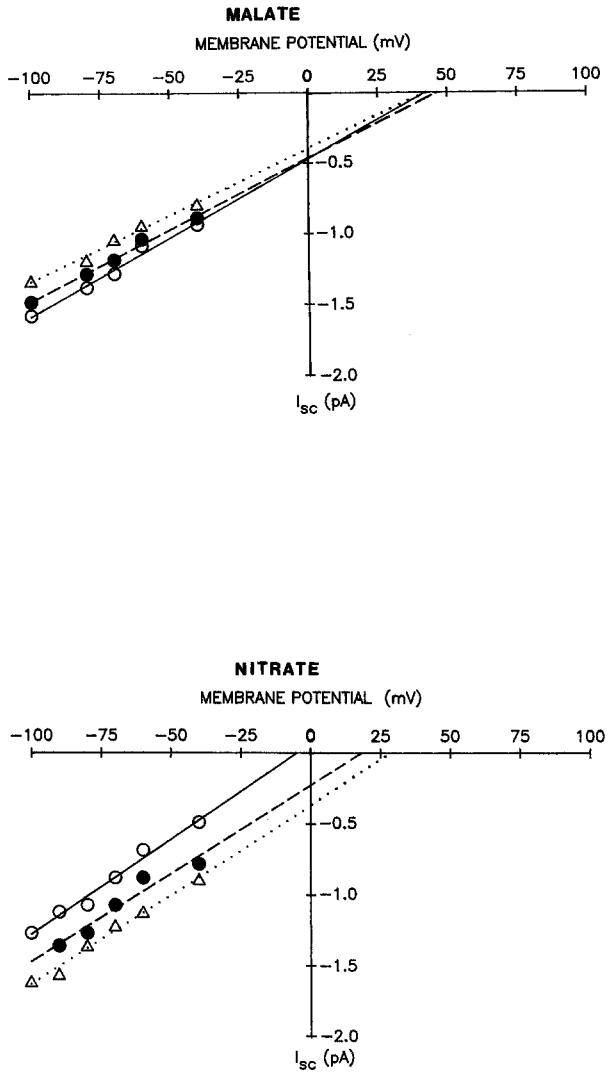

Fig. 7. Current-voltage relationships from single channels in isolated outside-out patches of the tonoplast. (*Upper panel*) Single channel currents were recorded with 50 mM malate in the cytoplasm and 5 mM malate in the vacuole, with 6 mM (○), 50 mM (●) and 100 mM (△) vacuolar chloride. Anion inward currents were recorded between 0 and −100 mV and the direction of channel openings reversed between +40 and +45 mV. (*Lower panel*) Single channel current-voltage plots were constructed from records under similar conditions in *A* but substituting malate for nitrate. Single channel currents (I_{sc}) reversed direction between −5 and +30 mV. The x-intercept of the least-squares fit line represents the reversal potentials (E_{rev}). Datapoints are the mean ± SE (n = 4).

HPO_4^{2-} (*data not shown*), the single channel conductance was still essentially unchanged (14.65, 16.61 and 6.73 pS for NO_3^-, Ac^- and HPO_4^{2-}, respectively) yet the magnitude of the single channel currents appeared to increase with the rise in Cl^-_{vac} concentrations. Increasing vacuolar chloride concentrations shifted the reversal potential (x-intercept) towards more positive values, more specifically towards the reversal potential for nitrate under the various chloride regimes.

Discussion

In moderate halophytes, the accumulation of chloride in vacuoles enables the plant to regulate cell turgor without expending energy in the synthesis of organic osmoregulants (Yeo, 1983). As our data suggest, vacuolar chloride may also be a factor in regulating anion transport across the tonoplast. In a previous study, we characterized a vacuolar anion channel with a high anion to cation selectivity ($P_{mal}/P_{K^+} > 6$). This channel was active at physiological pH conditions (cytoplasmic pH = 7.5; vacuolar pH = 6.0), cytoplasmic Ca^{2+} concentrations (lower than 10^{-6} M), and tonoplast potentials. A role for this channel mediating the influx of malate and other anions into the vacuole was postulated (Pantoja et al., 1992). Here, we report the regulation of this channel by intravacuolar chloride at the above mentioned conditions. At high vacuolar chloride concentrations, time-dependent inward currents across the tonoplast are stimulated to mediate the influx of nitrate, phosphate and acetate into the vacuole, while the influx of malate is reduced.

Nitrate and phosphate are major plant nutrients that are accumulated and stored in the vacuole from which they may be retrieved according to various metabolic demands (Granstedt & Huffaker, 1982). In contrast, the accumulation and storage of malate in C_3 plant vacuoles is not as physiologically significant as in C_4 and CAM plant vacuoles. In C_4 and CAM plants, malate serves as a major CO_2 source for photosynthetic processes, during the daytime for CAM plants and in the bundle sheath cells for C_4 plants (Lance & Rustin, 1984). In this respect, the physiological significance of the results presented in this work can be postulated. The activation of channel activity by chloride would provide a pathway for the storage of nutrients such as nitrate and phosphate into the vacuole, reflecting physiological aspects of maturing cells such as increased uptake of ions to build turgor and cause cell stretching (Hedrich & Schroeder, 1989). In addition, the reduction of the malate currents into the vacuole would allow the use of malate for mitochondrial oxidation and cytoplasmic pH control (Davies, 1986).

The mediating effect of chloride is reflected by the permeability sequences of the inward current at both low and high concentrations of vacuolar chloride. Malate becomes less permeable relative to the other anions, as the concentrations of chloride increase. The other anions, however, become increasingly more permeable, favoring their uptake and storage. With a mixed anion composition, as expected in the cytoplasm, it can be proposed that as the vacuolar chloride concentrations rise, acetate, nitrate and phosphate uptake will be selected for over malate. This is reflected in the shifts in reversal potentials towards their Nernst Equilibrium Potentials (E_{Nernst}) with nitrate, acetate and phosphate and the lack

of shift with malate, as the vacuolar chloride concentrations are increased. Such changes are not detected in the whole-vacuole configuration because chloride efflux through the instantaneous outward channels shifts the reversal potential towards E_{Nernst} for chloride, and the whole-vacuole configuration represents the average of all the currents, both inward and outward.

The increase in current for nitrate, acetate and phosphate by high vacuolar chloride is seen as an increase in the number of channel openings at a given tonoplast potential and a decrease in the time spent by the channel in the closed state. In the presence of chloride, conformational changes of the channel protein, which induce the transition from a closed state to an open state, may be catalyzed by an increased sensitivity of the voltage sensor and gating charges to electrical changes across the membrane (Hille, 1984). As a consequence of the lowering of the activation potential of the channel, the free-energy favoring the transition of the channel to the open state will decrease. The opposite is true when malate is present in solution.

These effects may be envisioned by assuming a conformational alteration to the voltage sensor of the ion channel. An electrostatic effect of chloride, screening fixed charges in the tonoplast, thus changing the tonoplast surface potential, cannot be ruled out. Halides, with the exception of fluoride, are chaotropic agents that have been shown to disrupt macromolecular interactions (Hatefi & Hanstein, 1969). Chaotrops, such as chloride, are able to exert their effect by altering the structure of water associated with macromolecules, thus weakening hydrophobic interactions and inducing changes in protein conformations (Dandliker & deSaussure, 1971). Chloride may be affecting the structural components of the channel on the vacuolar side, which in turn may have an effect on the voltage sensitivity of the channel gating mechanism that activates or inhibits the channel in response to stimulating voltages.

Although vacuolar chloride affected malate and nitrate (in addition to phosphate and acetate) currents in a differential manner, the similarities in voltage and time dependency, Zn^{2+} sensitivity, single channel conductances, and the apparent number of chloride ions needed for the activation or inhibition of nitrate and malate currents, respectively, would suggest a common anion channel mediating malate and nitrate currents.

In conclusion, the data presented here would support the notion of vacuolar chloride regulating vacuolar anion channel activity. High vacuolar chloride concentrations would favor the transport of nitrate, phosphate and acetate into the vacuole, while malate permeability would be reduced. The increase in vacuolar chloride concentrations also resulted in an increase in outward instantaneous currents. Although the physiological significance of these currents is not yet clear, it could be postulated that these currents allow the efflux of chloride from the vacuole into the cytoplasm, thus compensating for the expected hyperpolarization of the tonoplast due to nitrate (phosphate and acetate) influx. The coupling of anion fluxes into the vacuole with vacuolar chloride efflux is currently under investigation.

This work was supported by the National Science and Engineering Research Council of Canada.

References

Barry, P.H., Lynch, J.W. 1991. Liquid junction potentials and small cell effects in patch-clamp analysis. *J. Membrane Biol.* **121:**101–117

Bertl, A., Blumwald, E., Coronado, R., Eisenberg, R., Findlay, G., Gradmann, D., Hille, B., Koohler, K., Kolb, H.-A., MacRobbie, E., Meissner, G., Miller, C., Neher, E., Palade, P., Pantoja, O., Sanders, D., Schroeder, J., Slayman, C., Spanswick, R., Walker, A., Williams, A. 1992. Electrical measurements on endomembranes. *Science* **246:**873–874

Blumwald, E. 1987. Tonoplast vesicles as a tool in the study of ion transport at the plant vacuole. *Physiol. Plant* **69:**731–734

Blumwald, E., Poole, R.J. 1987. Salt adaptation in suspension cultures of sugar beet. Induction of Na^+/H^+ antiport activity in tonoplast vesicles by salt. *Plant Physiol.* **83:**884–887

Boller, T., Wiemken, A. 1986. Dynamics of vacuolar compartmentation. *Annu. Rev. Plant Physiol.* **37:**137–164

Coyaud, L., Kurdjian, A., Hedrich, R. 1987. Ion channels and ATP-driven pumps involved in ion transport across the tonoplast of sugar beet vacuoles. *Biochim. Biophys. Acta* **902:**263–268

Dandliker, W.B., deSaussure, V.A. 1971. Stabilization of macromolecules by hydrophobic bonding: Role of water structure and of chaotropic ions. *In:* The Chemistry of Biosurfaces. M.L. Hair, editor. pp. 1–43. Dekker, New York

Davies, D.D. 1986. The fine control of cytosolic pH. *Physiol. Plant* **67:**702–706

Franciolini, F., Petris, A. 1990. Chloride channels of biological membranes. *Biochim. Biophys. Acta* **1031:**247–259

Granstedt, R.C., Huffaker, R.C. 1982. Identification of the leaf vacuole as a major nitrate storage pool. *Plant Physiol.* **70:**410–413

Hamill, O.P., Marty, A., Neher, E., Sakmann, B., Sigworth, F.J. 1981. Improved patch-clamp techniques for high-resolution current recording from cells and cell-free membrane patches. *Pfluegers Arch.* **391:**85–100

Hatefi, Y., Hanstein, W.G. 1969. Solubilization of particulate proteins and nonelectrolytes by chaotropic agents. *Proc. Natl. Acad. Sci. USA* **62:**1129–1136

Hedrich, R., Kurkdjian, A. 1988. Characterization of an anion-permeable channel from sugar beet vacuoles: effect of inhibitors. *EMBO J.* **7:**3661–3666

Hedrich, R., Neher, E. 1987. Cytoplasmic calcium regulates voltage-dependent ion channels in plant vacuoles. *Nature* **329:**833–836

Hedrich, R., Schroeder, J.I. 1989. The physiology of ion-channels and electrogenic pumps in higher plants. *Annu. Rev. Plant Physiol.* **40:**539–569

Hedrich, R., Schroeder, J.I., Fernandez, J.M. 1987. Patch-clamp studies on higher plant cells: A perspective. *TIBS* **12:**49–52

Hille, B. 1984. Ionic Channels of Excitable Membranes. Sinauer Associates, Sunderland, MA

Labarca, P., Coronado, R., Miller, C. 1980. Thermodynamic and ki-

netic studies of the gating behavior of a K^+-selective channel from the sarcoplasmic reticulum membrane. *J. Gen. Physiol.* **76:**397–424

Lance, C., Rustin, P. 1984. The central role of malate in plant metabolism. *Physiol. Veg.* **21:**625–641

Lewis, C.A. 1979. Ion-concentration dependence of the reversal potential and the single channel conductance of ion channels at the frog neuromuscular junction. *J. Physiol.* **286:**417–445

Matile, P. 1978. Biochemistry and function of vacuoles. *Annu. Rev. Plant Physiol.* **29:**193–213

Neher, E. 1992. Ion channels for communication between and within cells. *Science* **256:**498–502

Pantoja, O., Dainty, J., Blumwald, E. 1989. Ion channels in vacuoles from halophytes and glycophytes. *FEBS Lett.* **255:**92–96

Pantoja, O., Dainty, J., Blumwald, E. 1992. Cytoplasmic chloride regulates cation channels in the vacuolar membrane of plant cells. *J. Membrane Biol.* **125:**219–229

Pantoja, O., Gelli, A., Blumwald, E. 1993. Voltage-dependent calcium channels in plant vacuoles. *Science* **255:**1567–1570

Pantoja, O., Gelli, A., Blumwald, E. 1992. Characterization of vacuolar malate and K^+ channels under physiological conditions. *Plant Physiol.* **100:**1137–1141

Sakmann, B. 1992. Elementary steps in synaptic transmission revealed by currents through single ion channels. *Science* **256:**503–512

Sakmann, B., Trube, G. 1984. Voltage-dependent inactivation of inward-rectifying single-channel currents in the guinea-pig heart cell membrane. *J. Physiol.* **347:**659–683

Tyerman, S.D. 1992. Anion channels in plants. *Annu. Rev. Plant. Physiol. Plant. Mol. Biol.* **43:**351–373

Wink, M. 1993. The plant vacuole: A multifunctional compartment. *J. Exp. Bot.* **44:**231–246

Yeo, A.R. 1983. Salinity resistance: physiologies and prices. *Physiol. Plant* **58:**214–222